Inorganic Chemistry

Article

pubs.acs.org/IC

Origin of Ferroelectricity in a Family of Polar Oxides: The Dion—Jacobson Phases

Nicole A. Benedek*

Materials Science and Engineering Program, The University of Texas at Austin, 1 University Station, Austin, Texas 78712, United States

Supporting Information

ABSTRACT: Recent work on layered perovskites has established the group theoretical guidelines under which a combination of octahedral distortions and cation ordering can break inversion symmetry, leading to polar structures. The microscopic mechanism of this form of ferroelectricity—so-called hybrid-improper ferroelectricity—has been elucidated in two families of layered perovskites: $AA'B_2O_6$ double perovskites and Ruddlesden−Popper phases. In this work, we use symmetry principles, crystal chemical models, and first-principles calculations to unravel the crystal chemical origin of ferroelectricity in the Dion−Jacobson phases, and show that the hybrid improper mechanism can provide a unifying explanation for the emergence of polar structures in this family of materials. We link trends in the magnitude of the induced polarizations to changes in structure and composition and discuss possible phase-transition scenarios. Our results suggest that the structures of several Dion−Jacobson phases that have previously been characterized as centrosymmetric should be re-examined. Our work adds new richness to theories of how polar structures emerge in layered perovskites.

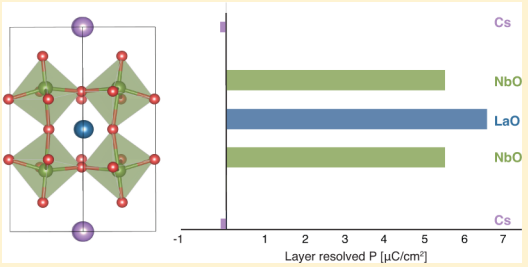

INTRODUCTION

The complex oxides are one of the largest and most technologically important inorganic materials families. The ABO_3 perovskite oxides in particular have been (and are still) the focus of intense research efforts because they display myriad fascinating physical properties,[1] including ferroelectricity, colossal magnetoresistance, metal−insulator transitions, and superconductivity. Although the details of the physical origin of these properties are often complicated, in many cases it is possible to identify simple guidelines or "rules of thumb" that link the property of interest to the structure and composition of the material. This knowledge, coupled with the development of sophisticated synthesis techniques, such as thin-film epitaxy[2] and topochemical approaches,[3,4] have given researchers the ability to precisely tailor the properties of perovskites for particular applications. Indeed, perovskites—and more broadly complex oxides—are a family of materials in which the paradigm of "materials-by-design" has been demonstrated very successfully.

Layered perovskite-like phases provide opportunities to further expand the functionality of perovskites. Perhaps the most well-known of these layered complex oxides are the Ruddlesden−Popper (RP) phases,[5,6] a homologous series of materials with general formula $A_{n+1}B_nO_{3n+1}$. A form of ferroelectricity was recently elucidated in the RP family, in which two nonpolar lattice distortions (rotations of the BO_6 octahedra) give rise to a polar structure. So-called hybrid-improper ferroelectricity[7,8] (a mechanism anticipated from the work of Woodward and co-workers[9−11]) gives researchers a great deal of compositional flexibility in designing new polar oxides[12−16] because most perovskites undergo octahedral rotation distortions.

There are other families of layered perovskites in addition to the RP phases, and it is natural to wonder whether there are hybrid-improper ferroelectrics among these other materials also. Like the RP series of materials, the Aurivillius phases[17] also feature stacks of perovskite-like blocks (with general formula $A_{n-1}B_nO_{3n+1}$), which are interleaved with Bi_2O_2 layers along the [001] direction.[18] The Aurivillius family contains a number of ferroelectric materials, some of which have been investigated[19,20] for their potential as fatigue-free ferroelectrics in nonvolatile memories. The B-site in many Aurivillius phases is commonly occupied by a so-called ferroelectrically active d^0 cation, such as Ti^{4+} or Nb^{5+}. However, Withers and co-workers[21] showed that the origin of ferroelectricity in the Aurivillius family is a gross underbonding at the perovskite A-site, which is relieved by a combination of octahedral rotations and polar distortions. Subsequent theoretical work by Perez-Mato et al.[22] revealed that the ferroelectricity in this class of materials emerges in a far more complex manner than in prototypical displacive ferroelectrics (such as $BaTiO_3$, for example), involving a number of both hard and soft polar and octahedral rotation modes.

The Dion−Jacobson (DJ) phases[23,24] have general formula $A'[A_{n-1}B_nO_{3n+1}]$ (for $n > 1$, the $n = 1$ member is ABO_4), where

Received: January 15, 2014
Published: March 28, 2014

   dx.doi.org/10.1021/ic500106a | Inorg. Chem. 2014, 53, 3769−3777

A′ separates the perovskite-like blocks and is typically a univalent alkali cation; see Figure 1. In contrast to the RP and

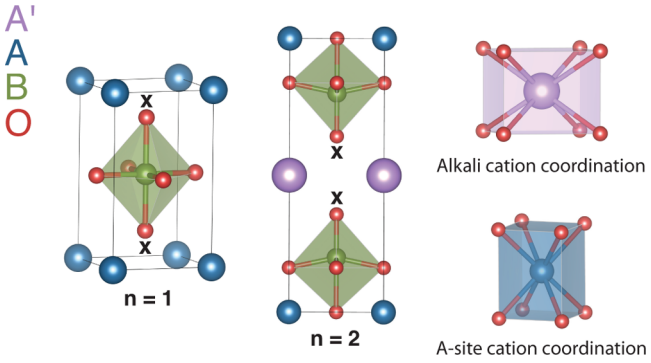

Figure 1. The structures of the $n = 1$ and $n = 2$ Dion–Jacobson phases in the $P4/mmm$ artistotype structure with coordination polyhedra for various atomic sites highlighted. The individual coordination polyhedra in the rightmost panel refer to the $n = 2$ Dion–Jacobson structure. The axial anions referred to in the text are denoted with an x.

Aurivillius families, the crystallography and properties of the DJ phases have not been as extensively investigated, which has led to a number of conflicting reports concerning the structures of various members of the family. Tantalizingly, however, previous work[25−28] on polar members of the DJ family has shown that these materials also undergo octahedral rotation distortions. Are there hybrid-improper ferroelectrics among the DJ phases?

In this work, we use first-principles density functional theory (DFT) calculations together with symmetry principles and crystal chemical models to explore the structures and properties of a series of $n = 2$ DJ phases. We present evidence suggesting that several DJ phases that have been experimentally characterized as having undistorted, nonpolar structures may actually undergo structural phase transitions to polar structures below room temperature. Our results suggest that the hybrid-improper mechanism can provide a unifying explanation for the emergence of polar structures in the DJ family, even though the DJ phases differ in their structure and crystal chemistry compared to previously studied hybrid-improper ferroelectrics. Similar to previously studied hybrid-improper ferroelectrics, the emergence of polar structures in the DJ phases is driven by octahedral rotation distortions, which optimize the A-site coordination environment. There is a large polarization arising from the A-site cation layers; however, in contrast to previously studied hybrid-improper ferroelectrics, the main contribution to the total polarization comes from the B–O layers. We link trends in the magnitude of the induced polarization to changes in structure and composition and discuss possible phase-transition scenarios.

STRUCTURES AND METHODS

Crystallography of the Dion–Jacobson Phases. Three aristotype structures are possible for the DJ phases, depending on the size and coordination preferences of the A and A′ cations.[29,30] If A or A′ is a large cation, such as Cs^+ or Rb^+, the perovskite blocks in adjacent layers are aligned, and the space group of the aristotype structure is $P4/mmm$, as shown in Figure 1. In this case, the axial anions indicated in Figure 1 are directly opposite each other; that is, they have the same xy coordinate but different z coordinates. When A or A′ is smaller, as in, for example, K^+, the perovskite blocks may "slip" by half a unit cell along the x or y axis only, in which case the space group of the aristotype structure is $Cmcm$. Finally, when the A′ cations (or A cations, for $n = 1$) are small—Li^+, Na^+, or Ag^+, for example—the perovskite blocks in adjacent layers along z may slip by half a unit cell along xy to minimize the electrostatic repulsion between the axial anions. In this case, the space group of the aristotype structure is $I4/mmm$. In this work, $n = 2$ DJ phases are considered with A′ = Cs and Rb; A = Y, Bi, La, and Nd; and B = Nb. The aristotype of relevance to this work is thus $P4/mmm$. Materials with composition $A'YNb_2O_7$ have not been synthesized in the DJ structure but are studied here to better understand structural trends across a series of compositions.

Analysis of Distorted Structures. Structures and structural distortions are analyzed using the symmetry-mode approach.[31−33] In this approach, distorted structures are related to a higher-symmetry reference or parent structure by atomic displacement patterns (modes) with certain symmetry properties. Let us take the mineral perovskite $CaTiO_3$ as an example. $CaTiO_3$ belongs to the orthorhombic $Pbnm$ (No. 62) space group at ambient temperatures but is thought to undergo a transition to the cubic $Pm\bar{3}m$ (No. 221) space group above 1600 K.[34] If $Pm\bar{3}m$ is selected as the space group of the reference structure ($Pm\bar{3}m$ is a suitable choice of parent space group regardless of whether $CaTiO_3$ actually undergoes the phase transition or not), then the subgroup $Pbnm$ can be reached by a combination of modes transforming like the irreducible representations (irreps) M_3^+ and R_4^+. The symmetry-allowed irreps can be easily enumerated for a given parent group–subgroup pair using readily available computer programs, such as ISOTROPY[35] or the Bilbao Crystallograhic Server.[36−38] How can we determine which distortions are energetically favorable, as opposed to merely symmetry-allowed? The energy E of the reference structure can be expanded in powers of small displacements to obtain (in one dimension),

$$E(u) = E^0 + \sum_n \frac{\partial E}{\partial u_n} u_n + \frac{1}{2} \sum_{n,m} \frac{\partial^2 E}{\partial u_n \partial u_m} u_n u_m \quad (1)$$

where E^0 is the energy of the unperturbed reference structure, u_n (u_m) is the displacement of atom n (m) from its equilibrium position in the reference structure, and the expansion is truncated at quadratic order. The linear term is the force on an atom and, by definition, vanishes for a reference structure at equilibrium. The coefficient of the quadratic term is defined as the force constant J.

$$J_{mn} \equiv \left(\frac{\partial^2 E}{\partial u_m \partial u_n} \right) \quad (2)$$

In three dimensions, the force constants form a $3N \times 3N$ matrix, where N is the number of atoms and the elements of the matrix are

$$J_{mn}^{\alpha\beta} = \frac{\partial^2 E}{\partial u_{m\alpha} \partial u_{n\beta}} \quad (3)$$

where $u_{m\alpha}$ is now the displacement of ion m in Cartesian direction α from its equilibrium position in the reference structure. The eigenvalues of this matrix are force constants corresponding to the displacements of modes, rather than of individual atoms; these modes are the eigenvectors of the force constants matrix. Hence, the force constants matrix essentially provides information about the curvature of the energy surface about the high-symmetry reference structure. If all of the eigenvalues (force constants) are positive, then the reference structure is stable toward displacements of the atoms, and the energy is at a (local, at least) minimum with respect to atomic displacements. However, if one (or more) of the force constants is negative, this indicates that the reference structure is unstable with respect to the particular mode with the negative force constant and that the energy is at a saddle point or local maximum; that is, the atomic displacements corresponding to the modes with the negative force constants will lower the energy of the reference structure (for small amplitudes of the displacements). Returning to the example of $CaTiO_3$ in the $Pm\bar{3}m$ reference space group, the force constants corresponding to the M_3^+ and R_4^+ modes are negative, indicating that atomic displacements corresponding to these modes will lower the energy. Note that although a negative force constant signifies a structural instability, the actual lowest-energy structure will in general also depend on terms in

dx.doi.org/10.1021/ic500106a | Inorg. Chem. 2014, 53, 3769−3777

eq 1 that are higher than quadratic order (anharmonic terms). For example, $CaTiO_3$ also has a ferroelectric instability in the cubic phase, which is suppressed by displacements of the Ca ions that accompany the octahedral rotation M_3^+ and R_4^+ modes.[39]

There is a subtlety here regarding the analysis of structural distortions from a theoretical perspective and the corresponding observation of structural distortions from an experimental perspective, that is, phase transitions. The theoretical framework described above cannot describe the dynamics of a phase transition, and indeed that is not the aim of this work. The aim is to elucidate, in a rigorous and quantitative way, the various factors that lead a particular material to adopt a certain structure and to establish a general crystal chemical theory for the DJ phases based on these factors. However, it is possible to obtain clues concerning probable ground state structures, intermediate phases, and phase-transition paths, particularly for structures that are simultaneously unstable to multiple modes and/or that undergo a sequence of phase transitions. This will be discussed further below.

First-Principles Calculations. The Vienna Ab initio simulation package (VASP)[40−43] was used to perform the first-principles calculations presented in this work. A planewave cutoff of 500 eV was used with a 6 × 6 × 4 **k**-point mesh and the PBEsol functional. A force convergence tolerance of 2.5 meV/Å was used for all structural relaxations. Force-constant matrices were calculated using finite differences, and the results were checked with those calculated using density functional perturbation theory. Projector augmented wave (PAW) potentials[44,45] were used to represent the ionic cores with the following states included in the valence for each element: $4s^24p^65s^1$ for Rb, $5s^25p^66s^1$ for Cs, $4s^24p^64d^15s^2$ for Y, $5s^25p^65d^16s^2$ for La, $4s^24p^64d^45s^1$ for Nb, and $2s^22p^4$ for O. For Nd we used a PAW potential in which three of the 4f electrons were frozen in the core, resulting in a valence configuration of $4f^15s^25p^66s^2$.

The total and layer-resolved polarizations $\mathcal{P}$ for each material in the $P2_1am$ structure were calculated using the expression[46]

$$\mathcal{P} = \frac{|e|}{\Omega}\sum_s Z_s^* \mathbf{u}_s \quad (4)$$

where $|e|$ is the electron charge, Ω is the unit cell volume, Z_s^* is the Born effective charge tensor of atom s in the $P4/mmm$ reference structure (calculated using density functional perturbation theory), and $\mathbf{u}_s$ is the displacement of atom s away from its position in the $P4/mmm$ reference structure. This is a linear approximation to the polarization, the fidelity of which has been explicitly verified for perovskites.[46]

Finally, when we speak of "ferroelectricity" we are referring to polar structures in which the displacements away from the reference structure are small and in which the polarization could, in principle, be switched to a symmetry-equivalent state.

RESULTS AND DISCUSSION

Evidence for Hybrid-Improper Ferroelectricity. In the RP and $ABO_3/A'BO_3$ double perovskite hybrid-improper ferroelectrics studied in references 7, 13, and 14, a combination of two different rotation patterns (analogous to the Glazer[47,48] $a^-a^-c^+$ rotation pattern in $Pbnm$ perovskites) establishes the polar ground state. In these families of materials, if the free energy $\mathcal{F}$ of the high-symmetry reference structure is expanded in powers of the polarization $\mathcal{P}$ and the two nonpolar modes R_1 and R_2, there is a term that trilinearly couples all three distortions:

$$\mathcal{F} \propto \mathcal{P}R_1R_2 \quad (5)$$

Fennie and Rabe showed,[26] using first-principles calculations, that $CsBiNb_2O_7$ is unstable to multiple distortions—Γ_5^-, M_2^+, and M_5^-—in a high-symmetry $P4/mmm$ reference structure. Figure 2 shows that a combination of the M_2^+ and M_5^- modes involve rotations of the oxygen octahedra, which double the unit cell in the ab plane and which, when combined, produce a rotation pattern analogous to the $a^-a^-c^+$ rotation pattern in bulk perovskites. The polar Γ_5^- mode involves mostly displacements of the Bi atoms. They noted that the space group of the polar room-temperature structure ($P2_1am$) could be reached from $P4/mmm$ by a combination of either the Γ_5^- and M_2^+ modes or the Γ_5^- and M_5^- modes; the stereochemical activity of the Bi lone pair was ultimately claimed to be the driving force for ferroelectricity. A third possibility (not explored by Fennie and Rabe) also exists: the M_2^+ and M_5^- modes. This possibility is the hallmark of hybrid-improper ferroelectricity in perovskites; that is, two nonpolar lattice modes establish the space group symmetry of the polar structure. Indeed, it is possible to expand the free energy of the $P4/mmm$ reference structure in terms of Γ_5^-, M_2^+, and M_5^- and obtain a trilinear term exactly as shown in eq 5. However, this symmetry analysis cannot tell us how much each distortion (or combination of distortions) will lower the energy across our series of materials, nor can it tell us about the magnitude of the polarization in the ground state. We calculated the force constants for the Γ_5^-, M_2^+, and M_5^- modes in the $P4/mmm$ reference structure for each material in our test set. Table 1 shows that all of the materials are unstable to at least the M_2^+ and M_5^- modes in the centrosymmetric $P4/mmm$ reference structure and that the polar $P2_1am$ structure is lower in energy than the $P4/mmm$, $Pmam$, $P4/mbm$, and $C2mm$ structures; that is, a structure that contains a combination of distortions is lower in energy than any of the distortions individually. Table 1 also shows that the magnitude of the polarization in the $P2_1am$ ground state for each material is significant and varies systematically with composition (the trend will be discussed in detail in the following section).

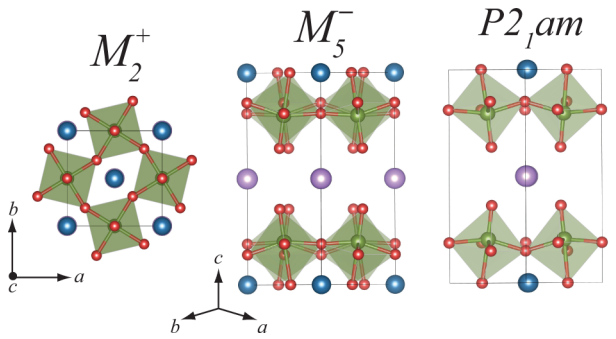

Figure 2. Schematic of the atomic displacements corresponding to the M_2^+ rotation and M_5^- rotation. The polar $P2_1am$ structure is also shown. Note that the M_2^+ rotation in this case is analogous to the Glazer $a^0a^0c^+$ rotation of the perovskite structure (and leads to space group No. 127 $P4/mbm$), whereas M_5^- is analogous to $a^-a^-c^0$ (and leads to space group No. 51 $Pmam$). Hence, the combined rotation pattern in $P2_1am$ is analogous to the $a^-a^-c^+$ pattern displayed by $Pbnm$ perovskites. Note that although they are not shown for clarity, the M_5^- mode also features displacements of the A′, A, and B cations.

$CsBiNb_2O_7$,[25,27] $RbBiNb_2O_7$,[28] and $CsNdNb_2O_7$[25] have been shown experimentally to adopt the $P2_1am$ structure at room temperature (we find excellent agreement between the experimentally reported structures and our calculated structures; see Supporting Information), but no unifying crystal chemical explanation for ferroelectricity in the DJ family has been offered. The stereoactive lone pair on Bi has been invoked to explain the polarity of the Bi-containing members, though as Table 1 shows, a steoreactive cation is not required. Snedden and co-workers[25] did note the role of the A-site cation

dx.doi.org/10.1021/ic500106a | Inorg. Chem. 2014, 53, 3769−3777

Table 1. Force Constants of Listed Modes for DJ Materials in the *P*4/*mmm* Space Group, Energy Difference (Per Formula Unit) between Fully Relaxed *P*4/*mmm* and Distorted Structures, and Total Macroscopic Polarization (in μC cm^{-2}) in the Polar $P2_1am$ Phase

	force constant [eV Å^{-2}]			ΔE [meV/f.u.][a]				polarization
material	Γ_5^-	M_2^+	M_5^-	*Pmam*	*P*4/*mbm*	*C*2*mm*[b]	$P2_1am$	[μC cm^{-2}]
$RbYNb_2O_7$	−3.765	−1.821	−4.303	−529	−444	−173	−1063	40
$RbNdNb_2O_7$	−0.866	−0.517	−2.347	−191	−69	−7	−349	30
$RbLaNb_2O_7$	0.285	−0.157	−1.272	−91	−6		−119	20
$RbBiNb_2O_7$	−7.900	−2.080	−6.862	−353	−406	−543	−814	48
$CsYNb_2O_7$	−3.847	−1.709	−4.276	−508	−388	−180	−1017	40
$CsNdNb_2O_7$	−1.003	−0.407	−2.368	−179	−39	−9	−320	29
$CsLaNb_2O_7$	0.595	−0.031	−1.258	−83	<−1		−102	18
$CsBiNb_2O_7$	−7.703	−1.941	−6.686	−338	−353	−553	−783	48

[a]A negative energy difference indicates that a structure with $P2_1am$ symmetry (or *C*2*mm*, *P*4/*mbm*, or *Pmam*) is more stable at zero Kelvin. [b]*C*2*mm* is the space group (No. 38) resulting from the freezing in of the Γ_5^- mode only along the tetragonal [110] direction.

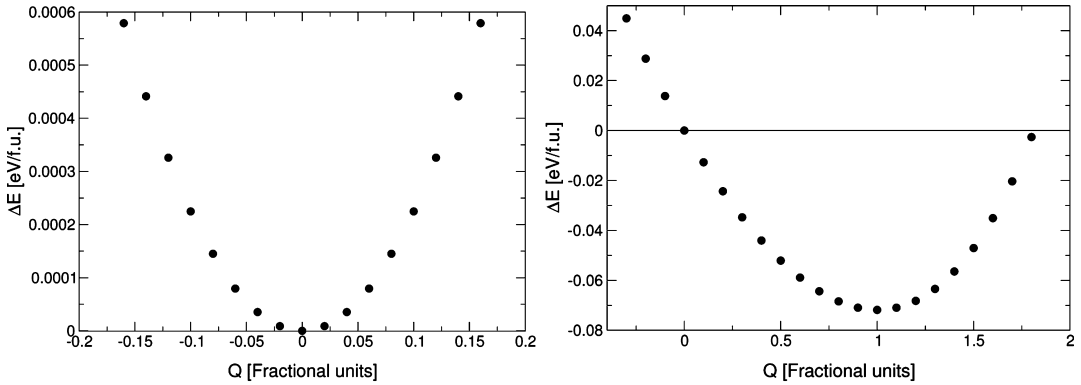

Figure 3. (a) Change in energy per formula unit of $CsLaNb_2O_7$ as a function of the amplitude *Q* of the polar Γ_5^- distortion. (b) Change in energy per formula unit of $CsLaNb_2O_7$ as a function of the polar Γ_5^- distortion in the presence of octahedral rotations. Note the differences in scale between the panels and also note that the zero of energy is different in each case. For (a), the zero of energy is the undistorted *P*4/*mmm* aristotype structure. For panel (b), the zero of energy is a structure with $P2_1am$ symmetry but no Γ_5^- distortion.

displacements and octahedral rotation distortions in driving polarity in the DJ phases. They also speculated as to why materials such as $CsLaNb_2O_7$ and $RbNdNb_2O_7$ have not been observed to display any structural distortion, even though "'tolerance factor' arguments would perhaps suggest"[25] that they should. Both $CsLaNb_2O_7$ and $RbLaNb_2O_7$ have only been reported in the *P*4/*mmm* structure (Gopalakrishnan and co-workers[29] suggested that $RbLaNb_2O_7$ may undergo octahedral tilting distortions, though their powder X-ray data did not indicate any unit cell doubling). $RbNdNb_2O_7$ was originally reported[49] in a 2 × *a* supercell but was later revised[50] to a simpler $a \approx 3.8$ Å, $c \approx 10.9$ Å subcell. Our results suggest that the structures of the La-containing compounds and $RbNdNb_2O_7$ should perhaps be re-examined at lower temperatures (our results for $RbNdNb_2O_7$ are in agreement with those of Sim and Kim, who also find that a polar structure with octahedral rotations is energetically favorable[51]). The La-containing materials are especially interesting because neither of them are unstable to Γ_5^- (or any zone-center) distortions; this indicates that the origin of ferroelectricity cannot be the same as that in proper ferroelectrics, such as $BaTiO_3$. Figure 3 shows how the energy of *P*4/*mmm* $CsLaNb_2O_7$ varies as a function of the Γ_5^- distortion only and Γ_5^- in the presence of the two rotation modes. The polar Γ_5^- distortion only lowers the energy in the presence of the rotations, and even then, the energy remains as a single well with the minimum at nonzero amplitudes of Γ_5^- (in contrast to the double-well potential characteristic of proper ferroelectrics; see Figure 3 of reference 8). In fact, all of the materials we considered display this same behavior, even the Bi-containing compounds, which have large Γ_5^- instabilities because of the stereoactive Bi^{3+} lone pair. Table 2 provides a summary of our findings in terms of which materials should be prepared and re-examined.

This behavior—polarization linear about zero and a single-well potential with a nonzero minimum—is a direct signature

Table 2. Summary of Findings for *n* = 2 Dion–Jacobson Phases Studied in This Work from Theory on Experiment

material	comments
$RbYNb_2O_7$, $CsYNb_2O_7$	polar ground state from theory; neither material has been previously synthesized
$RbNdNb_2O_7$, $CsNdNb_2O_7$	polar ground state from theory; $CsNdNb_2O_7$ polar from experiment;[25] $RbNdNb_2O_7$ nonpolar from experiment[49,50]
$RbLaNb_2O_7$, $CsLaNb_2O_7$	polar ground state from theory; both materials nonpolar from experiment[29]
$RbBiNb_2O_7$, $CsBiNb_2O_7$	polar ground state from theory; both materials polar from experiment;[25,27,28] polarization switching demonstrated for $RbBiNb_2O_7$[28]

dx.doi.org/10.1021/ic500106a | *Inorg. Chem.* 2014, 53, 3769–3777

of the trilinear coupling in eq 5. Hence, our results suggest that the hybrid-improper mechanism can provide a unifying explanation for the emergence of polar structures in the DJ family. This may seem like an obvious or foregone conclusion, given that the DJ family bears some structural resemblance (layered perovskite-like material) to the previously studied[7,13,14,52] double perovskite and RP hybrid-improper ferroelectrics. However, as we elaborate further below, the existence of a trilinear coupling in the free energy does not actually dictate anything about the crystal chemical origin of the polarization.

Crystal Chemical Origin of Polar Structures in the Dion—Jacobson Family. Previous work has shown that the $a^-a^-c^+$ rotation pattern in *Pbnm* perovskites induces an antiferroelectric displacement of the A-site cations. Although a polarization is induced in the A−O layers, the macroscopic polarization in bulk *Pbnm* perovskites is still zero because the A-sites are related by inversion symmetry through the B-site, which leads to a cancellation of the layer polarizations. When *Pbnm* perovskites are layered to create A-site ordered double perovskites[13] (with layered ordering of the A and A′ cations[15]) or RP phases,[14] then the A-sites are no longer related by inversion symmetry, the A−O layer polarizations are not exactly canceled, and a macroscopic polarization can arise, as shown in Figure 4 for the RP phase $Ca_3Mn_2O_7$.[7,8] Hence, in these materials ferroelectricity emerges from antiferroelectricity.

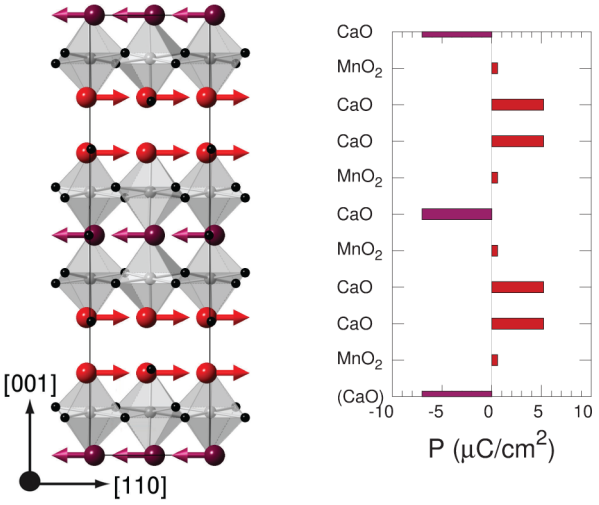

Figure 4. Layer-resolved polarization calculated from first principles for RP $Ca_3Mn_2O_7$. Red and magenta spheres are Ca ions (the two different colors are to distinguish the two different types of Ca ion), gray spheres are Mn, and black spheres are O. From reference 8, used with permission.

Not all hybrid-improper ferroelectrics display the mechanism described above. The free energy of the $PbTiO_3/SrTiO_3$ superlattices studied by Dawber and co-workers[52] features the same trilinear term shown in eq 5, where R_1 and R_2 are again octahedral rotation distortions. However, their combination does not form the $a^-a^-c^+$ rotation pattern displayed by double perovskites and RP phases, and thus there is no antiferroelectric displacement of the A-site cations. Instead, the polarization arises from a more conventional ($BaTiO_3$-like) displacement of the cation sublattice against the oxygen ions. Indeed, layering is not even a necessary requirement for the existence of hybrid-improper ferroelectricity.[53] Zhou and Rabe[54] showed that hybrid-improper ferroelectricity could be induced in epitaxially strained *bulk* $CaTiO_3$. In this case, the two nonpolar lattice modes R_1 and R_2 are not even octahedral rotation distortions.

Figure 5 shows the layer-resolved polarization for the $P2_1am$ phase of $CsLaNb_2O_7$. Like double perovskite and RP hybrid-

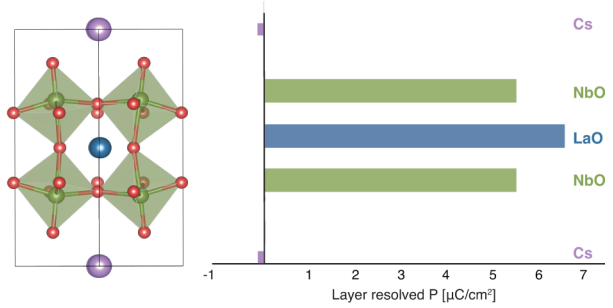

Figure 5. Layer-resolved polarization of $P2_1am$ $CsLaNb_2O_7$. The unit cell has been shifted along the z axis such that the Cs atoms are at z = 0. Note that there is only one Cs layer per crystallographic unit cell; the second layer shown above is a periodic image. The direction of both the bulk and A−O and B−O layer-resolved polarizations is parallel to the orthorhombic a axis, in agreement with previous work on polar DJ phases.[25−27]

improper ferroelectrics, there is a large polarization arising from the A−O layer. However, unlike double perovskites and RP phases, most of the macroscopic polarization is contributed by the B−O layers. It is tempting to conclude that this is due to a conventional ferroelectric mechanism, that is, charge transfer between the Nb d states and O p states, and that Nb−O hybridization is the real driver of ferroelectricity in this family of materials. However, as we will see, although this is a sufficient condition, it is not really necessary.

Figure 6 shows the contribution of each A−O and Nb−O layer to the total polarization for each material in our test set. We can make a number of points based on the data presented in Table 1 and Figure 6. First, the structures, bonding environments, and layer-resolved and total macroscopic

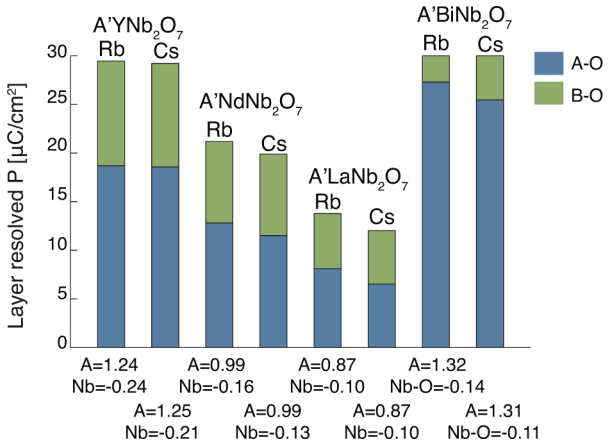

Figure 6. Layer-resolved A−O and Nb−O polarization for each material studied in the $P2_1am$ phase. For $RbYNb_2O_7$ for example, the A−O layer induces a polarization of ∼19 $\mu C/cm^2$, whereas each Nb−O layer induces a polarization of ∼11 $\mu C/cm^2$. The data along the x-axis is the discrepancy factor for the A-site cations and the Nb ions in valence units (v.u.) calculated for each material in the $P4/mmm$ reference structure.

dx.doi.org/10.1021/ic500106a | Inorg. Chem. 2014, 53, 3769−3777

polarizations are almost identical for both the Cs and Rb-containing DJ phases. The role of the alkali cations is to relieve electrostatic repulsion between the axial anions indicated in Figure 1, and once this electrostatic requirement has been satisfied, those cations are essentially inert spectator ions.

Second, the magnitude of the total polarization and A−O layer polarization in each material increases as the discrepancy factor of the A-site cation increases, that is, as the driving force for octahedral rotations increases. The discrepancy factor[55] is defined as the difference between an ion's formal valence and that calculated with the bond valence model, with a positive discrepancy factor indicating under-bonding. The A-site cations in all of the materials we considered are under-bonded in *P*4/*mmm*, sometimes (as in the case of the Y-containing compounds) severely so. This suggests that the transition to the polar state is driven by A-site bonding preferences, similar to RP phases and double perovskite hybrid-improper ferroelectrics. Further evidence for this hypothesis can be found by examining the form of the ferroelectric Γ_5^- eigenvectors of the *P*4/*mmm* reference structure. In all cases, the A-site cations make much larger displacements than the Nb or alkali cations. In particular, the A−O layer contribution for the Bi-containing compounds is much enhanced compared to the other materials because of the stereochemically active Bi^{3+} lone pair, as expected.[56−58] The polarization coming from the Nb−O layers never exceeds that coming from the A−O layers, but because there are two Nb−O layers per unit cell compared to only one A−O layer, with the exception of the Bi-containing materials, the main contribution to the total polarization comes from the Nb−O layers.

Unlike the A-site cations, our bond valence analysis shows that the Nb atoms in each of our materials are over-bonded (their discrepancy factors are negative). There is a much smaller variation in the discrepancy factors of the Nb atoms compared to the A-site cations, which lends further support to our claim that the origin of the polar structures in this family of materials is A-site under-bonding. The trend in the discrepancy factors of the Nb atoms as a function of the A-site cation is explained in Figure 7 (the much smaller variation in the discrepancy factors of the Nb atoms means that the trend is necessarily also rather subtle). In the *P*4/*mmm* reference structure the Nb atoms are octahedrally coordinated with four

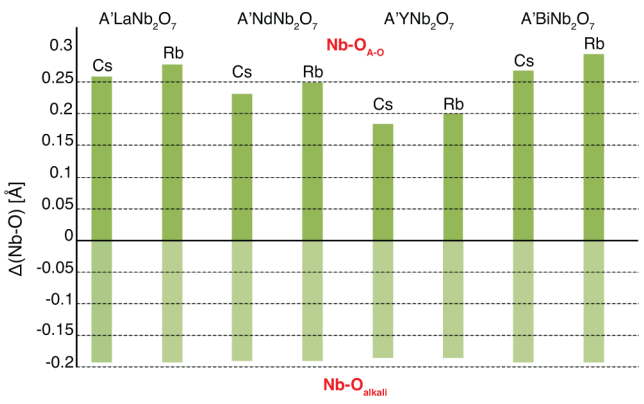

Figure 7. Difference between ideal Nb−O bond length in octahedral coordination from the bond valence model (1.9785 Å) and $Nb-O_{A-O}$ (top) and $Nb-O_{alkali}$ (bottom) for DJ phases in the *P*4/*mmm* reference structure. Both sets of bonds (slowly) approach zero as the A-site cation size decreases, but $Nb-O_{A-O}$ changes more quickly than $Nb-O_{alkali}$.

bonds of equal length to the equatorial oxygen atoms, one very short bond to the apical oxygen adjacent to the alkali cation ($Nb-O_{alkali}$), and one long bond to the apical oxygen in the A−O layer ($Nb-O_{A-O}$). The four equatorial bonds are closer to ideal length than are the $Nb-O_{alkali}$ and $Nb-O_{A-O}$ bonds. Although the Nb atoms in the La-containing compounds appear to be most optimally bonded (as evidenced by their small discrepancy factors), this is actually due to a "cancellation of errors," so to speak. $Nb-O_{A-O}$ contributes much less to the bond valence sum of Nb than is ideal, but this is made up by the much larger-than-ideal contribution of $Nb-O_{alkali}$, resulting in a discrepancy factor close to zero. For the Y-containing compounds, both $Nb-O_{alkali}$ and $Nb-O_{A-O}$ are closer to ideal. But the change in $Nb-O_{A-O}$ is not large enough to make up for the still very significant contribution to the bond valence sum coming from $Nb-O_{alkali}$, resulting in a discrepancy factor that is larger than in the La-containing compounds. (Since the bond valence of a bond changes exponentially with bond length, $Nb-O_{alkali}$ by itself contributes almost 30% to the bond valence sum of the Nb atoms.)

Although the polarization coming from the Nb−O layers could be enhanced by d(Nb)−p(O) hybridization, this is not a necessary condition for a polarization to arise. We tested this by performing calculations on $RbYSb_2O_7$. Sb^{5+} has a d^{10} electron configuration and therefore does not have states available to hybridize with the O p states. $RbYSb_2O_7$ is unstable to M_5^- and M_2^+ distortions in the high-symmetry *P*4/*mmm* reference structure, and the polarization of the material in the relaxed $P2_1am$ space group is 27 $\mu C/cm^2$, with each Sb−O layer contributing ∼7 $\mu C/cm^2$. Hence, a polarization can arise from the B−O layers even in the absence of a conventional chemical mechanism for ferroelectricity. Despite this, as far as we are aware there are no known DJ phases *without* a d^0 cation on the B-site. We wonder whether King and Woodward's[11] observation regarding the importance of ferroelectrically active cations in promoting A-site and B-site cation ordering in double perovskites may help to shed light on this situation. Although most ordered double perovskites and RP phases contain ferroelectrically active B-site cations, there are exceptions, for example, RP $Sr_3Sn_2O_7$[59] and double perovskite $KLaMgTeO_6$.[30] As a preliminary first step in exploring this phenomenon, in the Supporting Information we use $AA'B_2O_6$ double perovskites as a model system to show how the lattice topology can give rise to a significant B-site polarization in the absence of a ferroelectrically active cation. Although such an investigation was beyond the scope of this work, it would also be interesting to repeat the calculations and analysis described in this manuscript on the same series of materials, but with Nb replaced with Sb.

Before continuing we pause to note that, as with the previously studied and double perovskites and RP phases, the behavior of even-*n* DJ phases will differ from that of odd-*n* DJ phases. Specifically, as Aleksandrov and Bartolomé showed using a symmetry analysis,[60] the combination of rotation distortions that lead to a polar space group in even-*n* DJ phases will instead lead to a *nonpolar* space group for odd-*n* DJ phases. Note that this does not mean that it is impossible in principle for odd-*n* DJ phases to be polar, merely that the mechanism by which a polar structure emerges will not be the same as the mechanism for the even-*n* DJ phases.

Hybrid-Improper Ferroelectrics or Weak Ferroelectrics? Implications for Critical Behavior and Phase-Transition Sequence. As we have already discussed, the

dx.doi.org/10.1021/ic500106a | Inorg. Chem. 2014, 53, 3769−3777

ground-state polar structure of the n = 2 DJ phases is established by a combination of two different rotation patterns. This has implications for the phase transition from the high-symmetry $P4/mmm$ structure to the polar ground state. Two scenarios are possible: either both rotations condense simultaneously at the same temperature in a so-called avalanche transition[61] or one rotation pattern condenses, followed by the other one at a lower temperature. The former case would be a "true" improper ferroelectric transition, since the polarization is not the primary order parameter; the octahedral rotations, which arise at the zone-boundary of the high-symmetry reference structure form a coupled order parameter and simultaneously establish the polar ground state. In the latter case, the phase-transition sequence would be $P4/mmm \rightarrow Pmam$ or $P4/mbm \rightarrow P2_1am$. Here, the transition to the polar ground state from the intermediate state would actually be proper because, when the first rotation condenses, the unit cell will double, and the remaining rotation will be folded back to the zone-center of the new larger unit cell, where it will mix with the polar modes. We cannot definitively determine the phase-transition sequence with first-principles calculations alone, but we can obtain some clues as to probable intermediate structures. This is important because the experimental signatures and critical behavior of proper and improper ferroelectrics differ significantly, as discussed further below.

We consider the La-containing n = 2 DJ phases because Table 1 shows that although there is a strong M_5^- instability, the M_2^+ distortion is much weaker and barely lowers the energy of the $P4/mmm$ reference structure. This suggests that instead of a direct transition to the polar ground state, the transition may proceed through an intermediate $Pmam$ phase, which is connected to the polar $P2_1am$ ground state by a zone-center polar mode that transforms like the irrep Γ_3^-. We calculated the force constants for the Γ_3^- modes of $CsLaNb_2O_7$ and $RbLaNb_2O_7$ in the $Pmam$ phase and found unstable modes with force constants of -0.40 eV/Å^2 and -0.46 eV/Å^2, respectively. However, although Γ_3^- arises at the zone-center of the $Pmam$ phase and would therefore induce a proper ferroelectric transition, there is an important difference between this transition and that which occurs in conventional proper ferroelectrics, such as $BaTiO_3$. In materials like $BaTiO_3$, the ferroelectric transition is driven by a single zone-center optical phonon mode, which couples strongly to an external electric field as measured by its mode effective charge $\bar{Z}_j^*$.[62]

$$\bar{Z}_j^* = \sum_s \sqrt{M}_s Z_s^* \xi_{js} \tag{6}$$

where M_s is the mass of atom s, Z_s^* is the Born effective charge tensor of atom s in mode j, and ξ_{js} is the eigenvector of mode j. The mode effective charge of the ferroelectric mode in $BaTiO_3$ is 8.95 e.[62] In contrast, the mode effective charge of the unstable Γ_3^- mode of $Pmam$ $CsLaNb_2O_7$ is a paltry 0.20 e. Why is the mode effective charge of Γ_3^- so small compared to the polar mode in $BaTiO_3$, and why does this matter? Tagantsev and co-workers[63,64] coined the term "weakly polar" ferroelectrics to describe such materials and noted that "the small value of the effective charge of a soft mode of a weakly polar ferroelectric is a consequence of the circumstance that this mode has 'arrived' at the Γ point from the boundary of the Brillouin zone upon a transition (real or hypothetical) which involves a doubling of the unit cell and which occurs at a temperature higher than that of the ferroelectric transition."[64] In other words, in our case, when the M_5^- instability freezes in then the unit cell doubles in the ab plane. The M_2^+ mode (which is a zone-boundary mode of the $P4/mmm$ reference structure) then gets "folded back" to the zone-center of the new $Pmam$ structure, where it mixes with the Γ_5^- modes of $P4/mmm$ to produce the Γ_3^- modes of $Pmam$. We checked this by projecting the Γ_3^- modes of $Pmam$ $CsLaNb_2O_7$ onto the Γ_5^- and M_2^+ modes of the $P4/mmm$ reference structure. The Γ_3^- modes of $Pmam$ are indeed a mixture of the M_2^+ and Γ_5^- modes of $P4/mmm$. We note that the preceding analysis was for the La-containing compounds specifically and that other members of the DJ family, in particular those with strong zone-center instabilities, may display different critical behavior.

Tagantsev[64] also discussed the differences in the critical behavior of conventional and weakly polar ferroelectrics. In contrast to conventional ferroelectrics, weakly polar ferroelectrics have anomalously small Curie–Weiss constants, and in some cases, their polarization may change sign with temperature. In the case of improper ferroelectrics, it is possible to show[52,65] that as a function of temperature, the polarization goes according to $T_C - T$ (where T_C is the transition temperature) instead of $(T_C - T)^{1/2}$ as in conventional proper ferroelectrics. In addition, the dielectric constants of improper ferroelectrics show only a weak temperature dependence, with a small discontinuity at the transition temperature. (Goff and co-workers[27] noted in their study of $CsBiNb_2O_7$ that the dielectric constant was low and temperature-independent.) Regardless of whether the DJ phases studied here are hybrid-improper or weakly polar ferroelectrics, they will not display the same critical behavior as conventional proper ferroelectrics; this should be kept in mind in experimental studies of these materials.

CONCLUSIONS

We used first-principles calculations to show that octahedral rotations, together with A-site cation displacements, induce ferroelectricity in n = 2 DJ phases. These A-site displacements induce a significant polarization in the A–O layers. However, in contrast to the double perovskite and RP phases studied previously, the main contribution to the total polarization comes from the B–O layers in the DJ family (with the exception of the Bi-containing materials), because even though the individual B–O layer polarizations never exceed the A–O polarizations, there are two B–O layers per unit cell as opposed to only one A–O layer. Despite any differences in the structures and crystal chemistry between double perovskite, n = 2 RP, and n = 2 DJ phases, we showed that the emergence of polar structures in all three families of materials can be understood within a single phenomenological framework: that of hybrid-improper ferroelectricity. Given the diversity of structures and chemistries among the family of layered perovskite-like phases, the apparent ubiquity of this trilinear coupling mechanism is surprising and remarkable. A systematic study of a series of Aurivillius phases (such a study does not exist, as far as we are aware) may yet reveal further complexities and surprises. We hope our work stimulates further experimental studies of $CsLaNb_2O_7$, $RbLaNb_2O_7$, and $RbNdNb_2O_7$, which our results suggest may actually adopt polar structures below room temperature. The exploration of the possibilities for the design and discovery of functional layered perovskites has only begun, and we hope our work encourages further efforts in this exciting area.

dx.doi.org/10.1021/ic500106a | Inorg. Chem. 2014, 53, 3769–3777

■ ASSOCIATED CONTENT

Supporting Information

Atomic coordinates from first-principles calculations and a brief illustration of the manner in which the lattice topology can give rise to a significant B-site polarization in the absence of ferroelectrically active cations. This material is available free of charge via the Internet at http://pubs.acs.org/.

■ AUTHOR INFORMATION

Corresponding Author

*E-mail: nicole.benedek@austin.utexas.edu.

Notes

The authors declare no competing financial interest.

■ ACKNOWLEDGMENTS

The author acknowledges helpful discussions with Turan Birol, Craig Fennie, Arnab Sen Gupta, Megan Strayer, Venkat Gopalan, and Tom Mallouk. This work was supported by The Welch Foundation under Grant No. F-1803 and made use of high-performance computing facilities provided by the Texas Advanced Computing Centre (TACC).

■ REFERENCES

(1) Goodenough, J. B. *Rep. Prog. Phys.* **2004**, *67*, 1915−1993.
(2) Schlom, D. G.; Chen, L.-Q.; Pan, X.; Schmehl, A.; Zurbuchen, M. A. *J. Am. Ceram. Soc.* **2008**, *91*, 2429−2454.
(3) Schaak, R. E.; Mallouk, T. E. *Chem. Mater.* **2002**, *14*, 1455−1471.
(4) Sanjaya Ranmohotti, K. G.; Josepha, E.; Choi, J.; Zhang, J.; Wiley, J. B. *Adv. Mater.* **2011**, *23*, 442−460.
(5) Ruddlesden, S. N.; Popper, P. *Acta Crystallogr.* **1957**, *10*, 538−539.
(6) Ruddlesden, S. N.; Popper, P. *Acta Crystallogr.* **1958**, *11*, 54−55.
(7) Benedek, N. A.; Fennie, C. J. *Phys. Rev. Lett.* **2011**, *106*, 107204.
(8) Benedek, N. A.; Mulder, A. T.; Fennie, C. J. *J. Solid State Chem.* **2012**, *195*, 11−20.
(9) Knapp, M. C.; Woodward, P. M. *J. Solid State Chem.* **2006**, *179*, 1076−1085.
(10) King, G.; Thimmaiah, S.; Dwivedi, A.; Woodward, P. M. *Chem. Mater.* **2007**, *19*, 6451−6458.
(11) King, G.; Woodward, P. M. *J. Mater. Chem.* **2010**, *20*, 5785−5796.
(12) Halasyamani, P. S.; Poeppelmeier, K. R. *Chem. Mater.* **1998**, *10*, 2753−2769.
(13) Rondinelli, J. M.; Fennie, C. J. *Adv. Mater.* **2012**, *24*, 1961−1968.
(14) Mulder, A. T.; Benedek, N. A.; Rondinelli, J. M.; Fennie, C. J. *Adv. Funct. Mater.* **2013**, *23*, 4810−4820.
(15) Young, J.; Rondinelli, J. M. *Chem. Mater.* **2013**, *25*, 4545−4550.
(16) Balachandran, P. V.; Puggioni, D.; Rondinelli, J. M. *Inorg. Chem.* **2013**, *53*, 336Ð348.
(17) Aurivillius, B. *Ark. Kemi* **1949**, *1*, 463−480 499−512.
(18) Boullay, P.; Trolliard, G.; Mercurio, D.; Perez-Mato, J. M.; Elcoro, L. *J. Solid State Chem.* **2002**, *164*, 252−260.
(19) A-Paz de Araujo, C.; Cuchiaro, J. D.; McMillan, L. D.; Scott, M. C.; Scott, J. F. *Nature* **1995**, *374*, 627−629.
(20) Scott, J. F. *Phys. World* **1995**, *8*, 45−50.
(21) Withers, R. L.; Thompson, J. G.; Rae, A. D. *J. Solid State Chem.* **1991**, *94*, 404−417.
(22) Perez-Mato, J. M.; Aroyo, M.; García, A.; Blaha, P.; Schwarz, K.; Schweifer, J.; Parlinski, K. *Phys. Rev. B* **2004**, *70*, 214111.
(23) Dion, M.; Ganne, M.; Tournoux, M. *Mater. Res. Bull.* **1981**, *16*, 1429−1435.
(24) Jacobson, A. J.; Johnson, J. W.; Lewandowski, J. T. *Inorg. Chem.* **1985**, *24*, 3727−3729.
(25) Snedden, A.; Knight, K. S.; Lightfoot, P. *J. Solid State Chem.* **2003**, *173*, 309−313.
(26) Fennie, C. J.; Rabe, K. M. *Appl. Phys. Lett.* **2006**, *88*, 262902.
(27) Goff, R. J.; Keeble, D.; Thomas, P. A.; Ritter, C.; Morrison, F. D.; Lightfoot, P. *Chem. Mater.* **2009**, *21*, 1296−1302.
(28) Li, B.; Osada, M.; Ozawa, T. C.; Sasaki, T. *Chem. Mater.* **2012**, *24*, 3111−3113.
(29) Gopalakrishnan, J.; Bhat, V.; Raveau, B. *Mater. Res. Bull.* **1987**, *22*, 413−417.
(30) Knapp, M. C. Investigations into the Structure and Properties of Perovskites, Layered Perovskites, and Defect Pyrochlores. Ph.D. Thesis, The Ohio State University, 2006
(31) Stokes, H. T.; Hatch, D. M.; Wells, J. D. *Phys. Rev. B* **1991**, *43*, 11010.
(32) Hatch, D. M.; Stokes, H. T. *Phys. Rev. B* **2001**, *65*, 014113.
(33) Perez-Mato, J. M.; Orobengoa, D.; Aroyo, M. I. *Acta. Crystallogr., Sect. A* **2010**, *66*, 558−590.
(34) Kennedy, B. J.; Howard, C. J.; Chakoumakos, B. C. *J. Phys.: Condens. Matter* **1999**, *11*, 1479−1488.
(35) Stokes, H. T.; Hatch, D. M.; Campbell, B. J. *ISOTROPY Software Suite;* Brigham Young University: Provo, UT, 2007.
(36) Aroyo, M. I.; Perez-Mato, J. M.; Capillas, C.; Kroumova, E.; Ivantchev, S.; Madariaga, G.; Kirov, A.; Wondratschek, H. *Z. Kristallogr.* **2006**, *221*, 15−27.
(37) Aroyo, M. I.; Kirov, A.; Capillas, C.; Perez-Mato, J. M.; Wondratschek, H. *Acta. Crystallogr., Sect. A* **2006**, *62*, 115−128.
(38) Aroyo, M. I.; Perez-Mato, J. M.; Orobengoa, D.; Tasci, E.; de la Flor, G.; Kirov, A. *Bulg. Chem. Commun.* **2011**, *43*, 183−197.
(39) Benedek, N. A.; Fennie, C. J. *J. Phys. Chem. C* **2013**, *117*, 13339−13349.
(40) Kresse, G.; Hafner, J. *Phys. Rev. B* **1993**, *47*, 558.
(41) Kresse, G.; Hafner, J. *Phys. Rev. B* **1994**, *49*, 14251.
(42) Kresse, G.; Hafner, J. *Comput. Mater. Sci.* **1996**, *6*, 15.
(43) Kresse, G.; Furthmüller, J. *Phys. Rev. B* **1996**, *54*, 11169.
(44) Blochl, P. E. *Phys. Rev. B* **1994**, *50*, 17953.
(45) Kresse, G.; Joubert, D. *Phys. Rev. B* **1999**, *59*, 1758.
(46) Resta, R.; Posternak, M.; Baldereschi, A. *Phys. Rev. Lett.* **1993**, *70*, 1010−1013.
(47) Glazer, A. M. *Acta Crystallogr.* **1972**, *B28*, 3384−3392.
(48) Aleksandrov, K. S. *Kristallografiya* **1976**, *21*, 249−255.
(49) Dion, M.; Ganne, M.; Tournoux, M. *Rev. Chim. Min.* **1986**, 61−69.
(50) Kodenkandath, T. A.; Kumbhar, A. S.; Zhou, W. L.; Wiley, J. B. *Inorg. Chem.* **2001**, *40*, 710−714.
(51) Sim, H.; Kim, B. G. *arXiv:1311.4140 [cond-mat.mtrl-sci]* 2013.
(52) Bousquet, E.; Dawber, M.; Stucki, N.; Lichtensteiger, C.; Hermet, P.; Gariglio, S.; Triscone, J.-M.; Ghosez, P. *Nature* **2008**, *452*, 732−736.
(53) Bellaiche, L.; Íñiguez, I. *Phys. Rev. B* **2013**, *88*, 014104.
(54) Zhou, Q.; Rabe, K. M. *arXiv:1306.1839 [cond-mat.mtrl-sci]* 2013.
(55) Rao, G. H.; Bärner, K.; Brown, I. D. *J. Phys.: Condens. Matter* **1998**, *10*, L757−L763.
(56) Waghmare, U. V.; Spaldin, N. A.; Kandpal, H. C.; Seshadri, R. *Phys. Rev. B* **2003**, *67*, 125111.
(57) Payne, D. J.; Egdell, R. G.; Walsh, A.; Watson, G. W.; Guo, J.; Glans, P.-A.; Learmonth, T.; Smith, K. E. *Phys. Rev. Lett.* **2006**, *96*, 157403.
(58) Stoltzfus, M. W.; Woodward, P. M.; Seshadri, R.; Klepeis, J.-H.; Bursten, B. *Inorg. Chem.* **2007**, *46*, 3839−3850.
(59) Green, M. A.; Prassides, K.; Day, P.; Neumann, D. A. *Int. J. Inorg. Mater.* **2000**, *2*, 35−41.
(60) Aleksandrov, K. S.; Bartolomé, J. *Phase Transitions* **2001**, *74*, 255−335.
(61) Etxebarria, I.; Perez-Mato, J. M.; Boullay, P. *Ferroelectrics* **2010**, *401*, 17−23.
(62) Zhong, W.; King-Smith, R. D.; Vanderbilt, D. *Phys. Rev. Lett.* **1994**, *72*, 3618−3621.
(63) Smolenskiĭ, G. A.; Siniĭ, I. G.; Tagantsev, A. K.; Prokhorova, S. F.; Mikvabiya, V. D.; Vindsh, V. *Zh. Eksp. Teor. Fiz.* **1985**, *88*, 1020−1031.
(64) Tagantsev, A. K. *JETP Lett.* **1987**, *45*, 447−450.

(65) Levanyuk, A. P.; Sannikov, D. G. *Usp. Fiz. Nauk* **1974**, *112*, 561−589.

dx.doi.org/10.1021/ic500106a | *Inorg. Chem.* 2014, 53, 3769−3777